EVS30 Symposium
Stuttgart, Germany, October 9 - 11, 2017

Shift Process Control of a Novel Two-speed Automatic Mechanical Transmission for Battery Electric Vehicle

Jianwu Zhang[1], Benben Chai[1], Liangchen Wan[1], Chengqiang Liu[2], Lianhua Lin[2]

[1]*School of Mechanical Engineering, Shanghai Jiao Tong University, Shanghai, 200240, People's Republic of China. Email: chaibenben2014@sjtu.edu.cn*

[2] *Shandong Shifeng Group Co., LTD., Gaotang Country, Shandong Province, People's Republic of China.*

Summary

For improving drive performance and efficiency, a clutch-free two-speed automatic mechanical transmission is introduced to an electric vehicle. An overall and optimal shift control strategy is proposed for an electric drive 2AMT according to dynamic features in cooperation control between drive motor and shift mechanism. Compared with the conventional geared transmissions equipped with automatic clutches, the novel 2AMT is directly connected to the drive motor without any kind of clutches and its shift control algorithm is discussed. As an important part in the control system, the energy-saving shift schedule is investigated and established by dynamic programming method. Then, bench tests of the electric drivetrain including clutch-free 2AMT are conducted to testify the cooperation control shift process. Further, detailed information about dynamic modelling and simulation at different phases of the shift process is provided. During up and down shifting operations, especially in the gear meshing phase and the motor driving mode transform, considerable shift shock are avoided by the state feedback compensation of drive motor torque to suppress the driveline oscillations.

Keywords: electric vehicle, automatic mechanical transmission, motor torque control, 2-speed shift

1 Introduction

Battery electric vehicle is a promising solution to the development of zero-emission and low carbon transportation [1]. The majority of pure electric vehicles are equipped with a single reducer, in which the total gear ratio is chosen by searching to a trade-off between launch performance in standstill and economic drive-ability at high speed [2-4]. The large traction motors and high power inverters are employed to sustain the big torque demands and wide speed ranges [5-7]. Therefore, the 2-speed transmissions owning electric shift mechanisms are suitable for electric vehicles of comparable dynamic performance and powertrain cost with conventional ones [8-10].

Electric drive 2-speed automatic mechanical transmission (e-2AMT), compared with the hydraulic automatic transmission (AT) and dual clutch transmission (DCT), has the advantages of simple structure, reliable control, and easier industrialization. And the driving motor is easy to achieve fast and accurate speed

regulation due to smaller rotor moment of inertia, so the clutch can be saved. The driving motor is directly connected to the input shaft of the transmission, which is easier to realize the integrated design and control of drive motor and transmission.

2 Configuration of e-2AMT

The drive motor is directly connected with the input shaft of the 2AMT assembly and power to the middle shaft, two shift gears, synchronizer, output shaft, final reducer, differential, left and right half shaft and the rear wheels, as shown in Figure1 (a). The shift mechanism consists of brushless direct current (BLDC) motor, worm pair, cylindrical cam, fork and synchronizer as shown in Figure1 (b). The actuation motor is employed to drive the shift mechanical system to specified position as quick as possible.

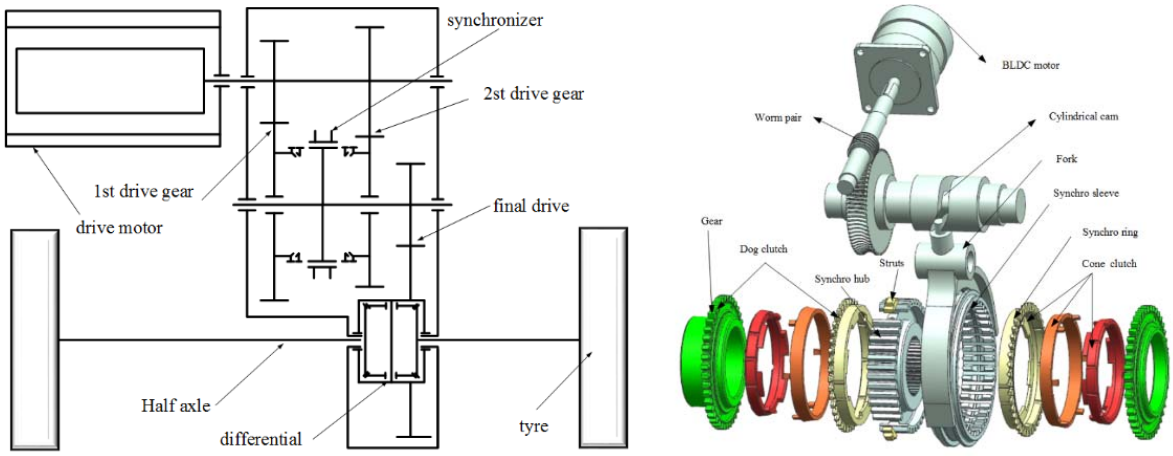

(a) Powertrain (b) shift actuator

Figure 1 Configuration of the powertrain and the shift actuator

3 Shift schedule of e-2AMT

The Dynamic Programming (DP) method is applied for design of the economical shift schedule to ensure the lowest oil consumption of the pure electric vehicles under certain driving cycle regulations.

For the first step, the DP algorithm according to the specific driving cycles, the demand torque $T_{t,k}$ of the drive wheel at discrete time sequence k can be expressed in the following formulas

$$T_{t,k} = \left(m \cdot g \cdot f + \frac{C_D \cdot A \cdot v_k^2}{21.15} + \delta \cdot m \cdot a_k \right) \cdot r_w \tag{1}$$

where m is mass of the vehicle, f is coefficient of rolling resistance, C_D is coefficient of air resistance, A is projection area, δ is inertia coefficient of the driveline components, and a_k is the acceleration, respectively. The regenerative braking torque of the drive motor is considered, and motor torque is obtained as:

$$T_{m,k} = \begin{cases} \dfrac{T_{t,k}}{i_0 \cdot i_{gi,k} \eta_T} & T_{t,k} \geq 0 \\ \dfrac{T_{t,k} \eta_T}{i_0 \cdot i_{gi,k}} & T_{t,k} < 0 \end{cases} \tag{2}$$

where $i_{gi,k}$ is gear ratio of 2AMT and i_0 is the final ratio. The traction motor speed is related to the vehicle velocity and presented in the following form:

$$n_{m,k} = \frac{30}{\pi} \cdot \frac{v_k}{3.6} \cdot i_{gi,k} \cdot i_0 \tag{3}$$

The efficiency map of the drive motor can be described by the implicit function of speed and torque as follows.

$$\eta_{m,k} = f\left(T_{m,k}, n_{m,k}\right) \tag{4}$$

Much effort is made in motor efficiency tests and statistics, as shown in Fig.2. The motor efficiencies are mapped into an ordered set of data in matrix form for easy applications. When the traction motor works to output or input, the power demanded for the battery pack $P_{mot\_dem,k}$ may be expressed in the following:

$$P_{mot\_dem,k} = \begin{cases} \dfrac{T_{m,k} \cdot n_{m,k}}{9550 \cdot \eta_{m,k}} \\ \dfrac{T_{m,k} \cdot n_{m,k}}{9550} \eta_{g,k} \end{cases} \tag{5}$$

In addition, the current of the battery can be determined according to the open circuit model of the battery as follows:

$$I_{Bat,k} = \frac{U_{oc,k} - \sqrt{U_{oc,k}^2 - 4 \cdot R_{Bat,k} \cdot P_{motor\_dem,k}}}{2 \cdot R_{Bat,k}} \tag{6}$$

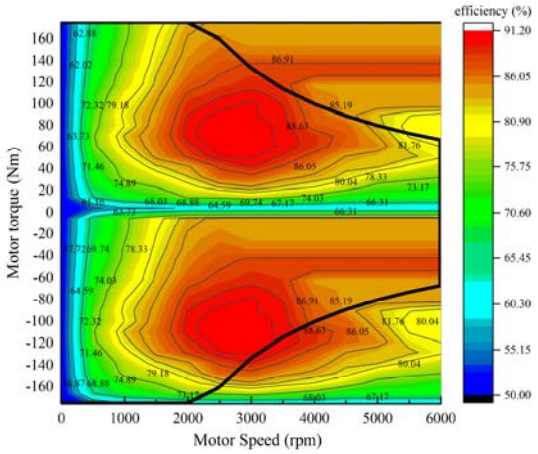

Figure 2 Efficiency map of drive motor

The Voltage-SOC and internal resistance-SOC correlative curves are given in Figure 3 and Figure 4.

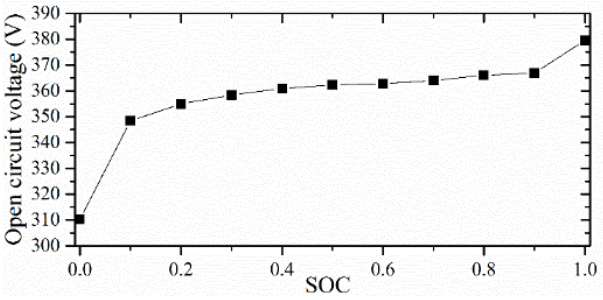

Figure 3 Battery voltage-SOC correlative curve

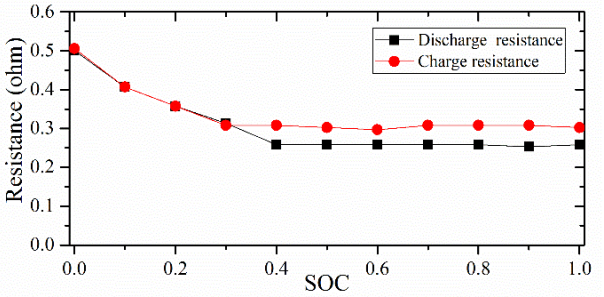

Figure 4 Battery internal resistance-SOC correlative curve

DP is a multistage decision process. Thus, in time series k, the state variable is chosen as State of Charge (SOC_k) of the battery, and the control variable is the gear state of transmission $i_{gi,k}$. During the optimization procedure, the inequality constraints are given to ensure safe and smooth operation of drive motor and battery.

$$\begin{cases} SOC_{\min} \le SOC_k \le SOC_{\max} \\ 0 \le T_{m,k} \le T_{\max,k}(n_{m,k}) \\ 0 \le n_{m,k} \le n_{\max} \\ 0 \le I_{\text{out},k} \le I_{Bat\_\max} \\ i_{gi,k} = \{1.32, 2.63\} \end{cases} \tag{7}$$

Further, state transform function is set below:

$$x_{k+1} = f_k(x_k, u_k) = SOC_k - \frac{I_{Bat,k}(i_{gi,k})}{Q_{Bat} \cdot 3600} \tag{8}$$

Since the energy economy considerations are important in design of the shift schedule. Frequently shift for the driver. Therefore, the penalty function of DP algorithm is defined as:

$$L_k(x_k, u_k) = \Delta u_k = \lambda \left| i_{gi,k+1} - i_{gi,k} \right| \tag{9}$$

So the cost function becomes

$$\min G = \min \sum_{k=0}^{N-1} (\Delta SOC_k + L_k) \tag{10}$$

For Step N :

$$G_N^* = 0 \tag{11}$$

For Step k , $0 \le k \le N-1$

$$G_k^*(SOC_k, i_{gi,k}) = \min \left\{ \Delta SOC_k + L_k + G_{k+1}^*(SOC_{k+1}, i_{gi,k+1}) \right\} \tag{12}$$

New European Driving Cycle (NEDC) and Japan 1015 Driving Cycle are taken as a basis of computation for the optimal control strategy in minimizing the cost function. The driving cycles and corresponding optimal gear shift sequence are plotted in Figure 5. Finally, the maximum overlapping area of gear optimal operation points of the two given driving cycles is drawn in Figure 6. The upshift schedule is the function of accelerator pedal throttle and vehicle speed and the downshift schedule is offset from the vehicle speed to avoid shift circle phenomenon. Using the above shift schedule, the energy consumption is saved 1.56% of NEDC and 2.28% of Japan 1015 compared to the shift schedule only obtained by vehicle speed.

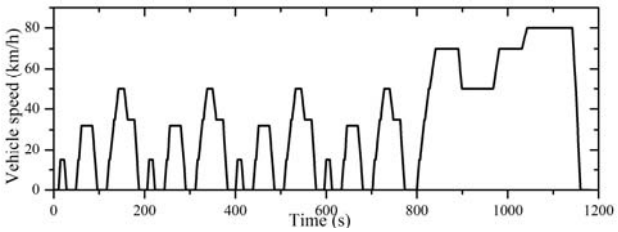

(a) New European Driving Cycle

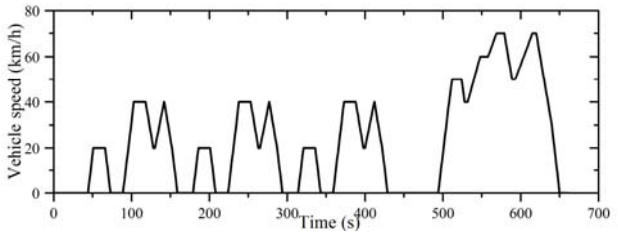

(b) Japan 1015 Driving Cycle

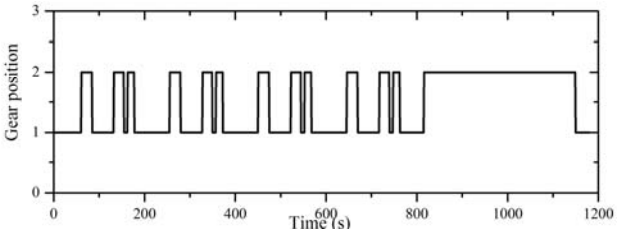

(c) Optimal gear control sequence in NEDC

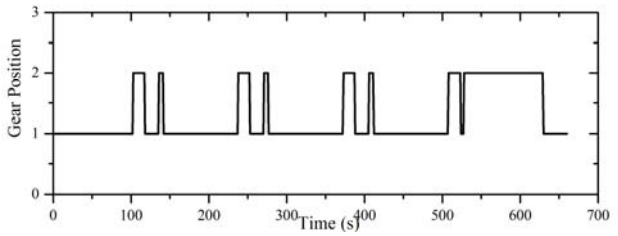

(d) Optimal gear control sequence in Japan 1015

Figure 5 Driving cycles and optimal gear shift sequence

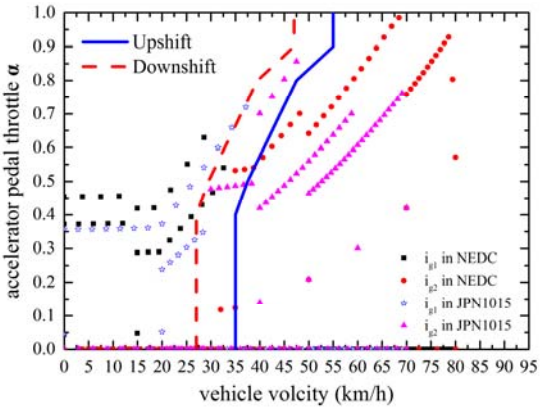

Figure 6 Optimal sequence of gear shifts

4 The cooperative control strategy of e-2AMT

Once the driver depresses the accelerator pedal, motor control unit (MCU) processes this signal into demand torque of the driver thus providing the corresponding voltage of the drive motor. The transmission control unit (TCU) decide to execute shift operation when the vehicle speed exceeds the previous value set at the current opening degree of the accelerator pedal. And during the shift process, TCU firstly send a signal to MCU to decrease the output torque for the purpose that the shift actuator can easily drive the fork arriving at the neutral position. Then active synchronizing of the target engaging gear will be employed by drive motor when TCU monitor encoder signal at the neutral position, decreasing the rotation speed of input shaft when upshift or increasing the speed when downshifting to match the output shaft. Next, the TCU will start the shift actuator again to drive the synchronizer to the target gear, engaging the output shaft with the target gear set when the active speed process finishes. Finally, the TCU will ask MCU to recover normal torque mode after the shift process.

As for the control of the shift motor, the general-purpose input-output (GPIO) of TMS320F28335 is used for controlling the BLDC rotating direction to realize upshift and downshift operation. Fork moving speed is regulated by changing the duty ratio of PWM of BLDC motor, and synchronizer axial position is indirectly monitored by counting quadrature pulse generating through the optical-electricity encoder mounted on the bottom of the BLDC motor. And the connection and control information of the e-2AMT assembly is shown in Figure 7.

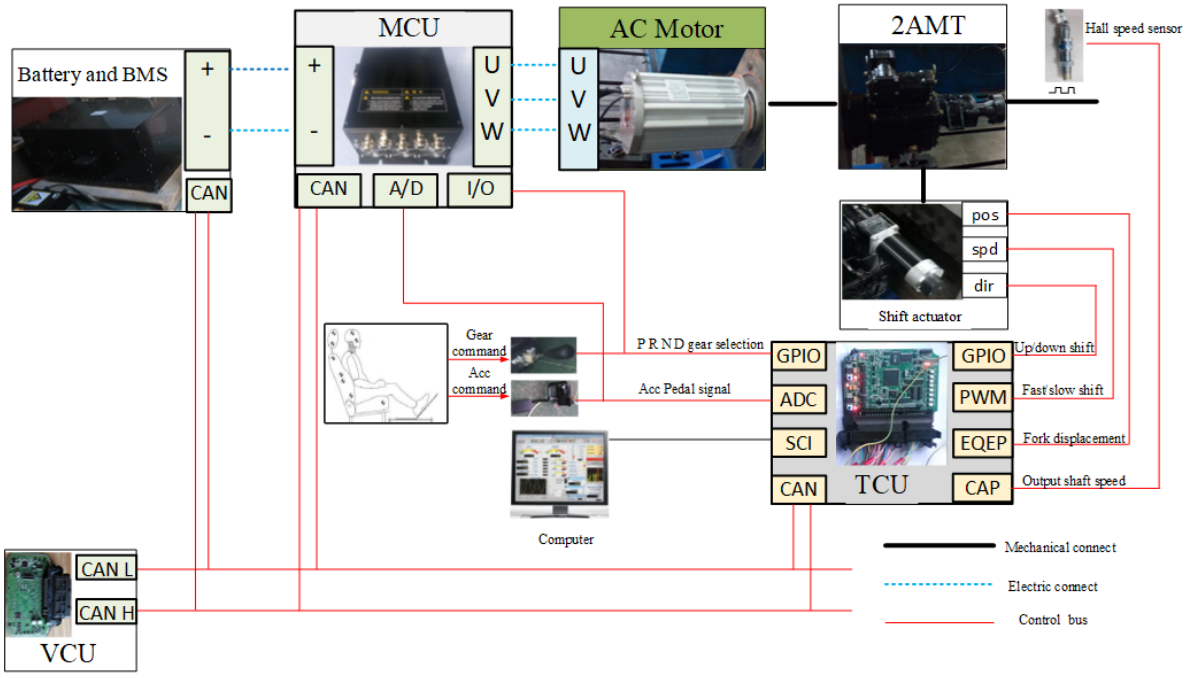

Figure 7 Control topology of e-2AMT

BMS: battery management system; CAN: controller area network; AC Motor: asynchronous motor; VCU: vehicle control unit; GPIO: general purpose input-output; PWM: pulse width modulation; EQEP: enhanced quadrature encoder pulse; e-CAP: enhanced capture module; ADC: analogue to digital converter; SCI: serial communication interface.

5 Dynamic model of shift process

The shifting process of e-2AMT without a clutch can be divided into seven phases: (1) decreasing the driving torque of AC motor; (2) disengaging the current gear; (3) electric synchronization by adjusting the AC motor speed to match the target gear; (4) free fly before mechanical synchronization; (5) mechanical synchronization with cone clutch; (6) engaging the target gear; (7) restoring driving torque of the AC motor. For the analysis of dynamic behaviours of torque transmission in each of the seven phases, the dynamics model of e-2AMT driveline is simplified and depicted in Figure 8.

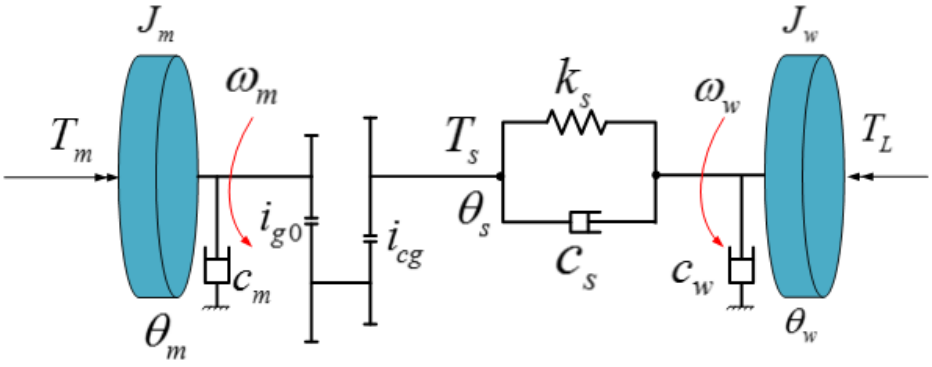

Figure 8 The dynamic model for e-2AMT

Accordingly, equilibriums equations of motion governing torsional vibrations of the driveline of two degree of freedom can be expressed in the following forms

$$J_m \dot{\omega}_m = T_m - c_m\omega_m - \frac{T_s}{i_{g0}i_{cg}} \tag{13}$$

$$J_w \dot{\omega}_w = T_s - c_w\omega_w - T_L \tag{14}$$

where ω_m and ω_w are drive motor and car wheel speeds, θ_s is torsional angle of the drive shaft, i_{g0} is gear ratio of constant meshed gear pairs, i_{cg} is gear ratio of current meshed gear pair, c_m , c_w and c_s are equivalent damping coefficient to the drive motor, car wheel and drive shaft, J_m is inertial moment of AC motor, J_w is moment inertial of wheels including car body effects, T_m is the drive motor torque, T_L is the longitudinal torque due to rolling resistance and air drag acting on the moving vehicle.

The torques acting on the drive shaft in different phase of the shift process can be written down as follows:

$$T_s = \begin{cases} k_s(\dfrac{\theta_m}{i_{g0}i_{cg}} - \theta_w) + c_s(\dfrac{\omega_m}{i_{g0}i_{cg}} - \omega_w) \ , \ s_{sl} = \pm s_0 \ ; \ \text{phase 1\&7} \\ \mu_0 F_{fork} R_r \ , \ -s_0 < s_{sl} < 0; \quad \text{phase 2} \\ 0 \qquad , \qquad s_{sl} = 0 \quad ; \quad \text{phase 3} \\ \mu_0 F_{fork} R_r \ , \ 0 < s_{sl} < s_{sl,syn}; \quad \text{phase 4} \\ -sign(\omega_w - \dfrac{\omega_m}{i_{g0}i_{cg}}) \dfrac{\mu_c F_{fork} R_r}{\sin\alpha_s}, s_{sl} = s_{sl,syn}; \text{phase 5} \\ F_{fork} R_r \dfrac{1\text{-}\mu_b \tan\varphi}{\mu_b + \tan\varphi}, \quad s_{sl,syn} < s_{sl} < s_0; \qquad \text{phase 6} \end{cases} \tag{15}$$

where k_s and c_s are stiffness and damping coefficient of the drive shaft, μ_0 is friction coefficient between hub and sleeve teeth of the synchronizer, F_{fork} is shifting force applied by the fork, R_r , s_{sl} , α_s and φ are engagement radius , displacement ,conic angle and chamfer angle of the synchronizer, μ_c and μ_b are friction coefficient of cone face and chamfer ,respectively.

6 Bench test

In order to evaluate the shift control algorithm of e-2AMT for EVs, a test bench is developed as shown in Figure 9. The bench consists of a high-voltage battery, MCU, a drive motor, an e-2AMT assembly including shift mechanisms, drive shaft, and load motor. A torque-speed sensor is mounted between the drive shaft and load motor to measure the torque and speed. The bench is capable of simulating the basic performance of an AMT electric control system on a real vehicle.

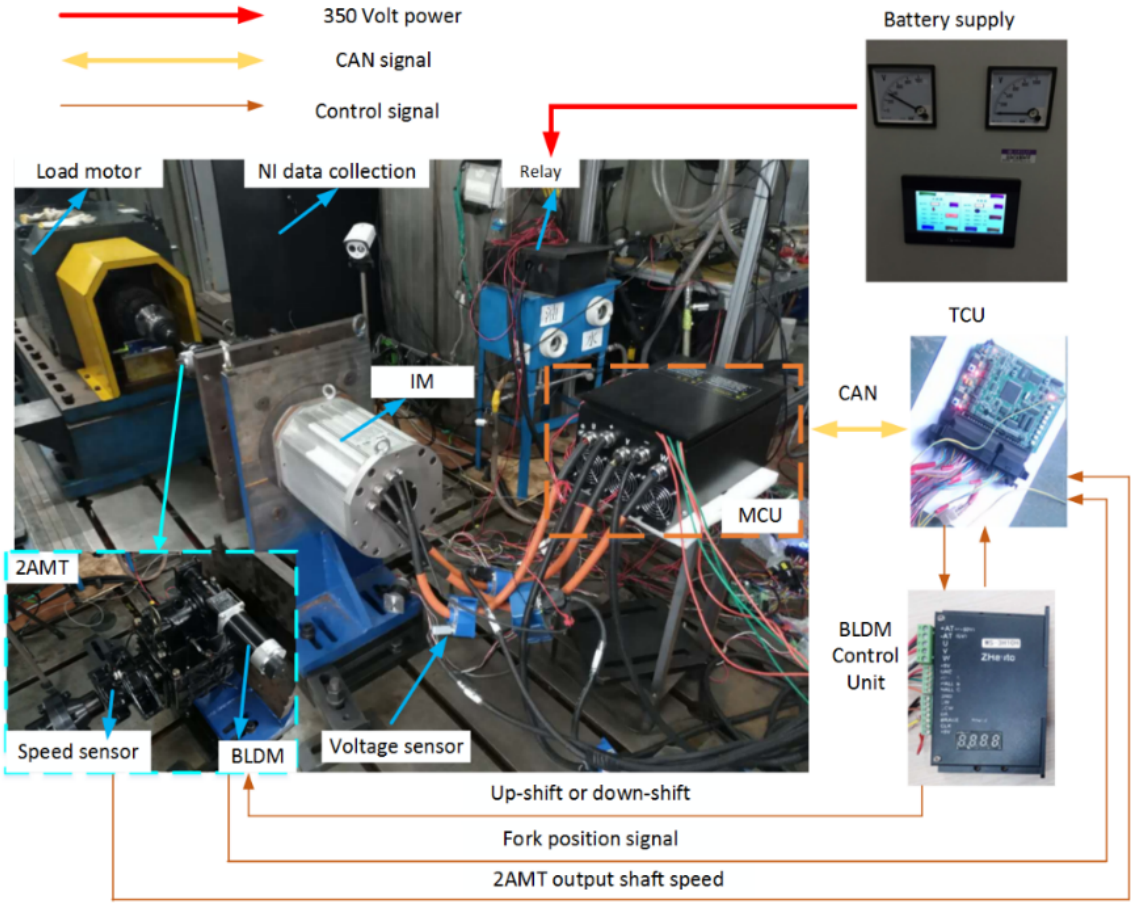

Figure 9 Test Bench for the e-2AMT, drive motor and dynamometer

7 Simulation and experiment results analysis

The entire shift process is established in MATLAB/SIMULINK. And simulations and experiments result of upshift and downshift process is shown in Figure 10 and Figure 11. The upshift operation is undertaken at 20% of full accelerate pedal with the motor speed of 2600 rpm and downshift with the motor speed of 600 rpm.

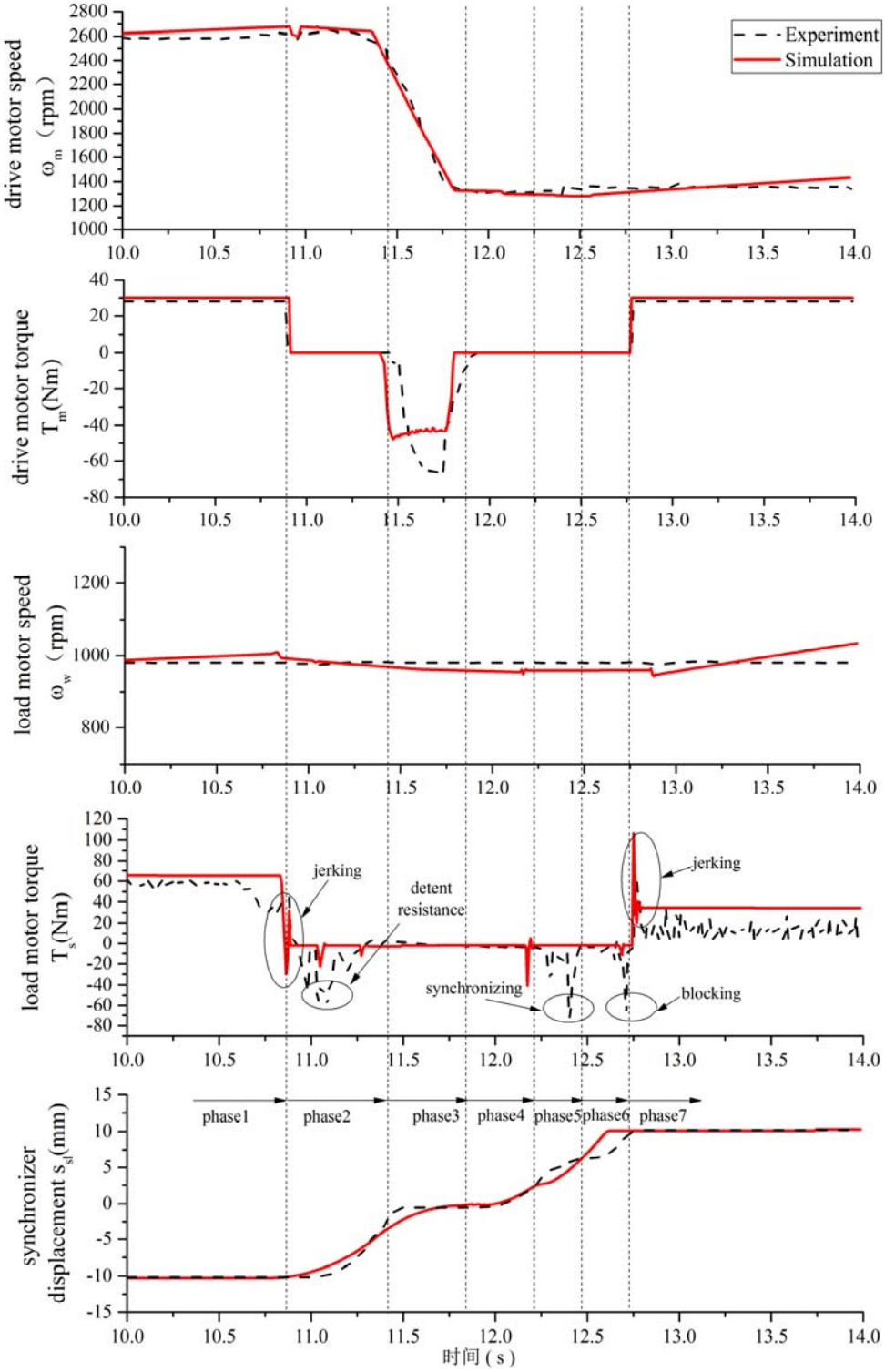

Figure 10 The upshift process of e-2AMT

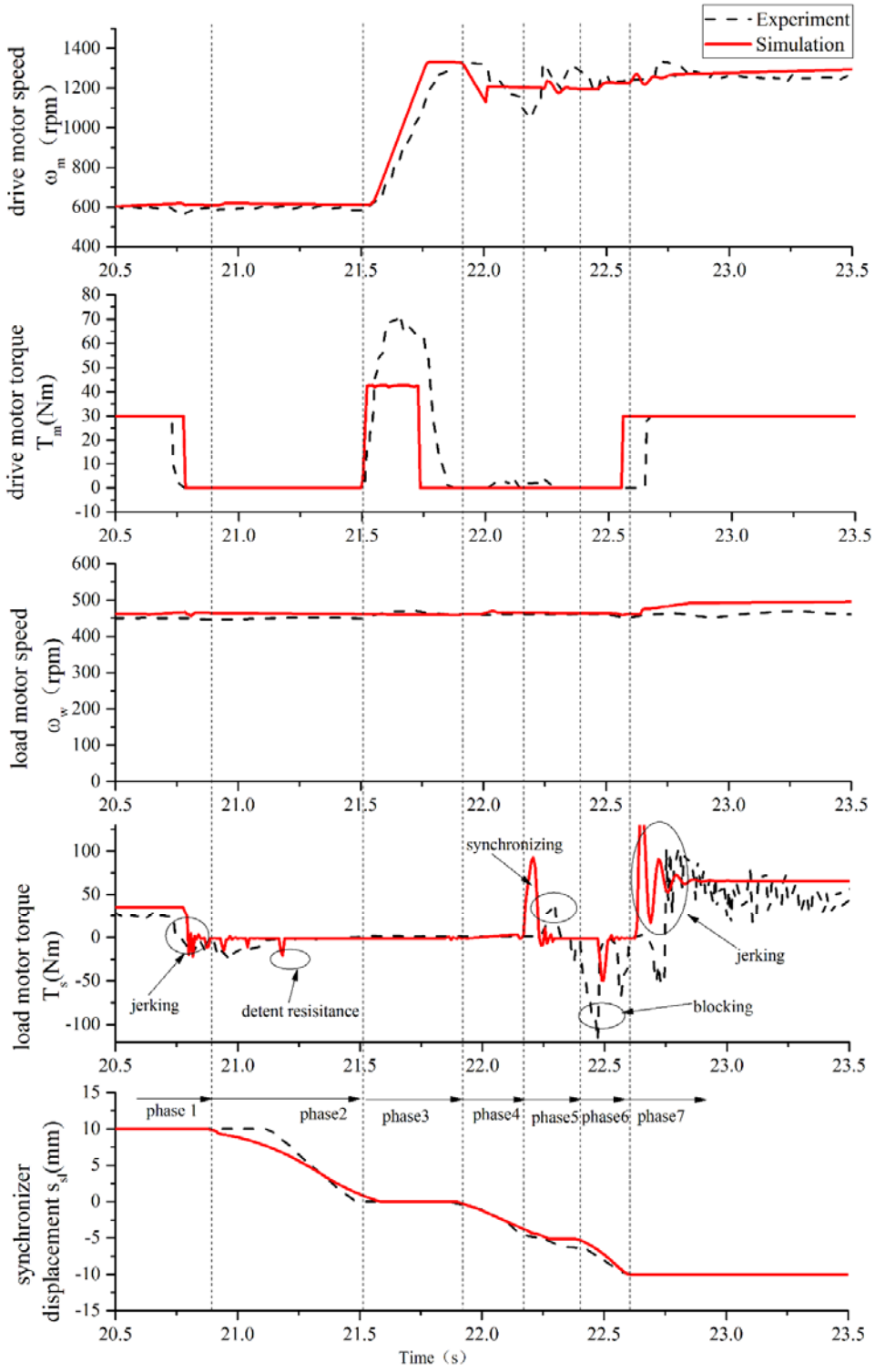

Figure 11 The downshift process of e-2AMT

And the detailed information of drive motor speed, load motor speed, drive motor torque, load motor torque and synchronizer displacement are present also. From the comparison of simulation and experiment result, the dynamic model of the driveline and shift actuator testify well with actual processes. And the seven phases of the shift process is clearly shown according to the synchronizer displacement and drive motor torque change. When the drive motor releases its torque to zero, the torque of the load motor will change sharply

due to the step impulse. The jerking problems will not only influence the drivability of vehicles, but also cause the oscillation of the output shaft of the transmission, which will influence the shift actuator movement thus increasing the shift time. Therefore, the first order resonance frequency analysis of the driveline and the active control of the drive motor are essential to improve the shift performance as well as decreasing resistance for shift actuator.

Specifically, for analysis of driveline during up and down shifts jerking phenomena, the equilibrium equations of motion of the driveline can be rewritten in matrix form as:

$$\begin{bmatrix} \dot{\omega}_m \\ \dot{\omega}_w \\ \dot{T}_s \end{bmatrix} = \begin{bmatrix} -\frac{c_m}{J_m} & 0 & -\frac{1}{J_m i_{cg} i_{g0}} \\ 0 & -\frac{c_w}{J_w} & \frac{1}{J_w} \\ \frac{k_s}{i_{cg} i_{g0}} & -k_s & 0 \end{bmatrix} \begin{bmatrix} \omega_m \\ \omega_w \\ T_s \end{bmatrix} + \begin{bmatrix} \frac{1}{J_m} \\ 0 \\ 0 \end{bmatrix} T_m + \begin{bmatrix} 0 \\ -\frac{1}{J_w} \\ 0 \end{bmatrix} T_L \tag{16}$$

Introducing of state variables into Eq. (16) results in the state equation of the following form as:

$$\dot{x} = Ax + Bu + Hl \tag{17}$$

Imposion of Laplace's transform to Eq.(17) leads to the transfer function of the driveline system:

$$\frac{T_s}{T_m} = \frac{J_w c_s s^2 + (J_w k_s + c_s c_w)s + k_s c_w}{a_1 s^3 + a_2 s^2 + a_3 s + a_4} \tag{18}$$

where

$$a_1 = i_{cg} i_{g0} J_m J_w$$

$$a_2 = (J_m + \frac{1}{i_{cg}^2 i_{g0}^2} J_w) i_{cg} i_f c_s + i_{cg} i_{g0} (J_m c_w + J_w c_m)$$

$$a_3 = (J_m + \frac{1}{i_{cg}^2 i_{g0}^2} J_w) i_{cg} i_{g0} k_s + (c_m + \frac{1}{i_{cg}^2 i_{g0}^2} c_w) i_{cg} i_f c_s + i_{cg} i_{g0} c_m c_w$$

$$a_4 = (c_m + \frac{1}{i_{cg}^2 i_{g0}^2} c_w) i_{cg} i_{g0} k_s$$

From Figure 12, it can be seen that the gear ratio will change the resonance frequency. When the transmission is at first gear, the resonance frequency is lower but the resonance peak is higher. Once the resonance frequency is excited, the jerking will be transmitted from the chassis to the drive, reducing the drivability of the vehicle.

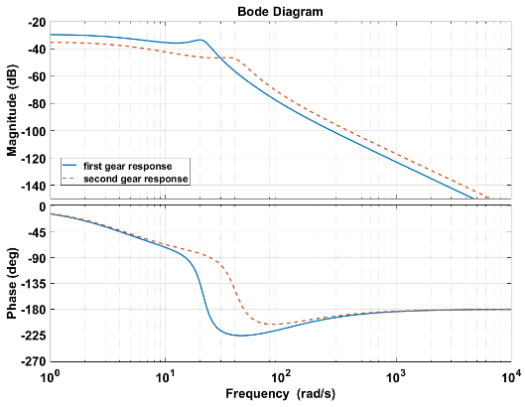

Figure 12 Bode diagram of the transfer function of the driveline

For design of a semi-active controller for applying damping forces to depress jerking of the driveline, the functional problem is established by the Linear Quadratic Regulator (LQR) approach as follow:

$$J = \int_0^\infty (x^T Q x + u^T r u) dt \tag{19}$$

And then the controller may be solved and presented in the following form as

$$u = -r^{-1} B^T P x = K_{optiaml} x \tag{20}$$

where P is the solution to the corresponding Riccati Equation

$$PA + A^T P - PBr^{-1} B^T P + Q = 0 \tag{21}$$

In which, Q and r are weighting coefficient matrices.

$$Q = \begin{bmatrix} q_1 & 0 & 0 \\ 0 & q_2 & 0 \\ 0 & 0 & 0 \end{bmatrix} \tag{22}$$

However, the LQR is model based control algorithm, the gear ratio should be considered when design the state feedback controller. So the controller implementation is shown as Figure 13. The speed of drive motor is referred to get the demand torque at current accelerator pedal opening, and the oscillation torque is calculated by the feedback gain $K_{optimal}$ multiply the state feedback value.

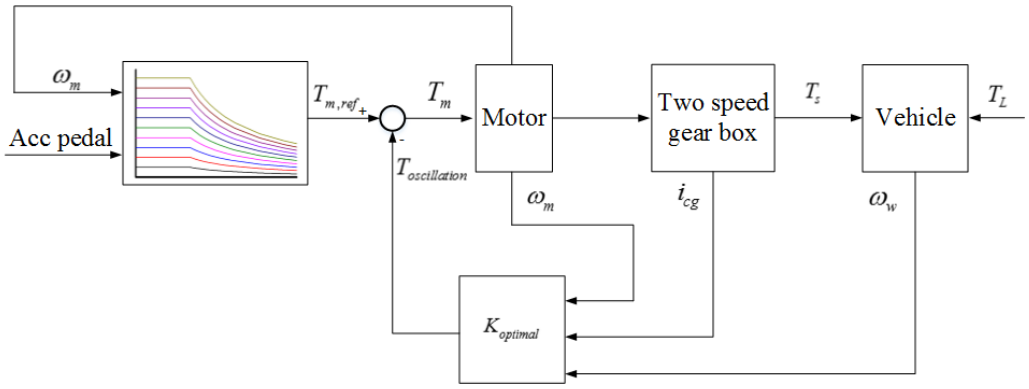

Figure 13 Block diagram of the LQR controller

The simulation results of the proposed control algorithm are shown in Figure 14 and Figure 15. The optimal gain are respectively $K_{optimal1} = [516 \quad -200 \quad 0]$ and $K_{optimal2} = [1320 \quad -1000 \quad 0]$. And the when at first gear, the driveline resonance frequency is lower and the amplitude is higher.

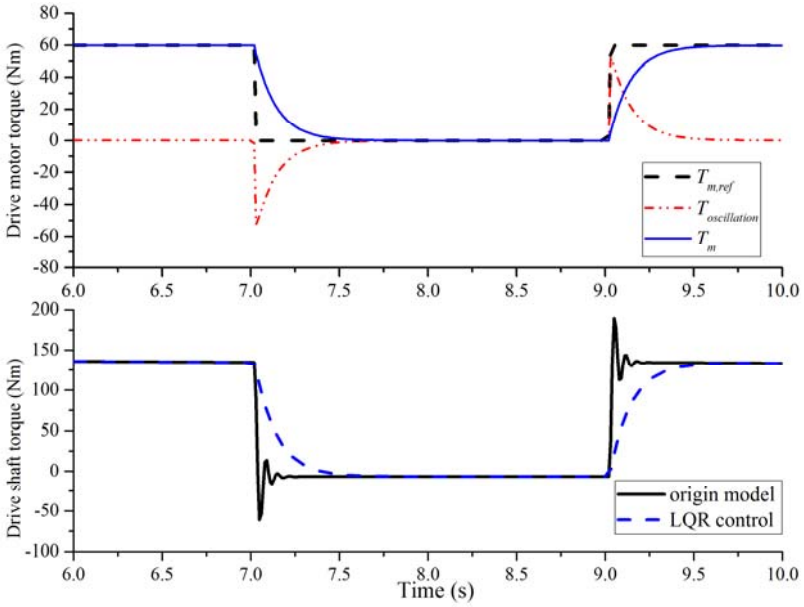

Figure 14 Simulation results of time domain responses for the drive motor and shaft torques using LQR controller in first gear shifting

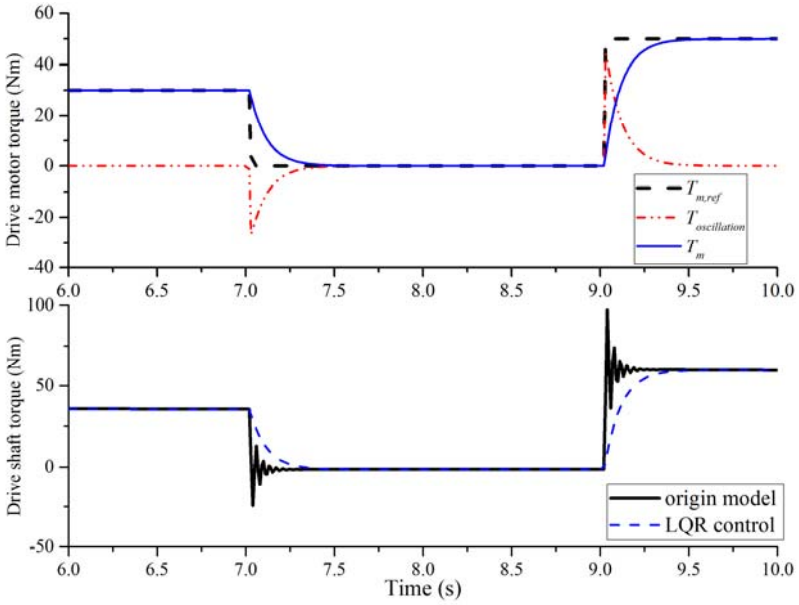

Figure 15 Simulation results of time domain responses for the drive motor and shaft torques using LQR controller in second gear shifting

8 Conclusion

With regard to the proposed e-2AMT equipped on electric vehicles, the energy-saving shift schedule is addressed by using dynamic programming (DP) method under typical driving cycles. Then, cooperation control of the drive motor and shift actuator is designed to realize smooth and fast shift process. Through the comparison with the bench test, the detailed seven phases shift process is testified well. Finally, in order to damp the jerking occurred during the drive motor torque changes, the LQR controller is applied and the oscillations can be well suppressed.

Acknowledgment

This reward work was financially supported by Major Special Science and Technology Projects Shandong Province, Government of P.R. China. (Grant Contract No.2015ZDXX0601C01).

Reference

[1] Ruan J, Walker P, Zhang N. A comparative study energy consumption and costs of battery electric vehicle transmissions [J]. Applied Energy, 2016, 165: 119-134.

[2] Di Nicola F, Sorniotti A, Holdstock T, et al. Optimization of a multiple-speed transmission for downsizing the motor of a fully electric vehicle[J]. SAE International Journal of Alternative Powertrains, 2012, 1(2012-01-0630): 134-143.

[3] Walker, P., B. Zhu, and N. Zhang, Powertrain dynamics and control of a two-speed dual clutch transmission for electric vehicles. Mechanical Systems and Signal Processing, 2017. 85: pp. 1-15.

[4] Gao B, Liang Q, Xiang Y, et al. Gear ratio optimization and shift control of 2-speed I-AMT in electric vehicle [J]. Mechanical Systems and Signal Processing, 2015, 50: 615-631.

[5] Tseng C Y, Yu C H. Advanced shifting control of synchronizer mechanisms for clutchless automatic manual transmission in an electric vehicle[J]. Mechanism and Machine Theory, 2015, 84: 37-56.

[6] Lin S, Chang S, Li B. Improving the gearshifts events in automated manual transmission by using an electromagnetic actuator[J]. Proceedings of the Institution of Mechanical Engineers, Part C: Journal of Mechanical Engineering Science, 2015, 229(9): 1548-1561.

[7] Yu C H, Tseng C Y. Research on gear-change control technology for the clutchless automatic–manual transmission of an electric vehicle [J]. Proceedings of the Institution of Mechanical Engineers, Part D: Journal of Automobile Engineering, 2013, 227(10): 1446-1458.

[8] Templin, P. and B. Egardt. An LQR torque compensator for driveline oscillation damping. in 2009 IEEE Control Applications, (CCA) & Intelligent Control, (ISIC). 2009.

[9] Kawamura, H., K. Ito, T. Karikomi, et al., Highly-Responsive Acceleration Control for the Nissan LEAF Electric Vehicle. 2011. 1.

[10] Kim, Y.-K., H.-W. Kim, I.-S. Lee, et al., A Speed Control for the Reduction of the Shift Shocks in Electric Vehicles with a Two-Speed AMT. Journal of Power Electronics, 2016. 16(4): pp. 1355-1366.

Authors

Jianwu Zhang received his PHD in Mechanical Engineering from Shanghai Jiao Tong University, Shanghai, China, in 1984. He became a Professor of Vehicle Engineering at Shanghai Jiao Tong University in 1992. His research interests include design, and control for advanced powertrain systems, particularly for the 2AMT of the electric vehicles.

Benben Chai received his BS in Vehicle Operation Engineering from Jilin University, Changchun, China, in 2014. He is currently a PHD candidate at Shanghai Jiao Tong University. His research interests include modelling and control of electric vehicles, torsional vibration control as well as TCU design.